# ACOUSTIC RAY TRACING WITH THE CONNECTION MACHINE

C. Sullivan, Y. Wang, and R.A. Kline
University of Oklahoma
School of Aerospace and Mechanical Engineering
865 Asp Avenue
Norman, Oklahoma 73019-0601

R.B. Mignogna and R.S. Schechter
Mechanics of Materials Branch
Naval Research Laboratory
Washington, D.C. 20375-5000

P.P. Delsanto and L. Ferrero
Dipartimento di Fisica
Politecnico di Torino
10129 Torino, Italy

## INTRODUCTION

Acoustic rays do not travel in straight raypaths in nonhomogeneous media. This causes difficulty in tomographic image reconstruction. A method for acoustic ray tracing in nonhomogeneous media has been developed using the parallel processing capabilities of the Connection Machine. This method of ray tracing is intended to facilitate a parallel processing approach to tomographic image reconstruction.

The computer simulation introduces a point source displacement into a two-dimensional specimen and the consequent displacements are calculated at every gridpoint, for each time increment. The location of the first arrivals are noted for each time step and correlate to the location of the wavefront. The normals of the wavefronts are calculated to define the raypath. Results from an isotropic three-layered medium and an Epstein layer ( a medium with a continual variation in material properties ) are compared with the raypath predictions obtained using Fermat's principle and Snell's law.

## PARALLEL PROCESSING TECHNIQUES

The two-dimensional specimen is divided into a grid of N by M cells as shown in

*Review of Progress in Quantitative Nondestructive Evaluation, Vol. 12*
Edited by D.O. Thompson and D.E. Chimenti, Plenum Press, New York, 1993

figure 1. Each cell has a one-to-one correspondence with the Connection Machine processors. Different material properties can be assigned to individual cells, or as in this case, to a layer of cells. The propagation of the wave motion is "taught" to each cell by means of an iteration equation, [1] as discussed below.

For a two-dimensional problem, the wave equation

$$\partial(S_{klmn} w_{m,n})_l = \rho \ddot{\omega} \tag{1}$$

can be written as

$$\begin{aligned} \rho\ddot{u} &= (\lambda+2\mu)\frac{\partial^2 u}{\partial x^2} + \mu\frac{\partial^2 u}{\partial y^2} + (\lambda+\mu)\frac{\partial^2 v}{\partial x \partial y} \\ \rho\ddot{v} &= (\lambda+2\mu)\frac{\partial^2 v}{\partial y^2} + \mu\frac{\partial^2 v}{\partial x^2} + (\lambda+\mu)\frac{\partial^2 u}{\partial x \partial y} \end{aligned} \tag{2}$$

Where $S_{klmn}$ is the stiffness tensor, w is the displacement vector, $\rho$ the is density, $\lambda$ and $\mu$ are Lamé constants and u and v are the x and y components of the displacement.

As described in reference [2], the wave equation (2) is transformed into finite difference equations

$$\begin{aligned} u_{i,j,t+1} &= \alpha(u_{i-1,j,t}+u_{i+1,j,t}) + \beta(u_{i,j-1,t}+u_{j+1,t}) - 2\xi u_{i,j,t} - u_{i,j,t-1} \\ &\quad + \gamma(v_{i-1,j-1,t}+v_{i-1,j+1,t}+v_{i+1,j-1,t}+v_{i+1,j+1,t}) \\ v_{i,j,t+1} &= \beta(v_{i-1,j,t}+v_{i+1,j,t}) + \alpha(v_{i,j-1,t}+v_{i,j+1,t}) - 2\xi v_{i,j,t} - v_{i,j,t-1} \\ &\quad + \gamma(u_{i-1,j-1,t}+u_{i-1,j+1,t}+u_{i+1,j-1,t}+u_{i+1,j+1,t}) \end{aligned} \tag{3}$$

where $u_{i,j,t}$ and $v_{i,j,t}$ correspond to the x and y displacements at a gridpoint (i,j) at time (t). Also

$$\alpha = \left(\frac{v_L}{\epsilon/\delta}\right)^2 \quad \beta = \left(\frac{v_T}{\epsilon/\delta}\right)^2 \quad \gamma = \alpha + \beta - 1$$

$$v_L = \sqrt{(\lambda+2\mu)/\rho} \qquad v_T = \sqrt{\mu/\rho} \tag{4}$$

where $\delta$ is the designated time increment.

## METHOD

The propagation medium in this study is treated as a two-dimensional, isotropic, and non-homogeneous material. The inhomogeneity stems from parallel layers with different material properties. The specimen is divided into a grid with each cell or grid point assigned a processor for computing purposes. The Lame constants, $\lambda$ and $\mu$, and a value for the density are assigned for the different layers. The finite difference form of

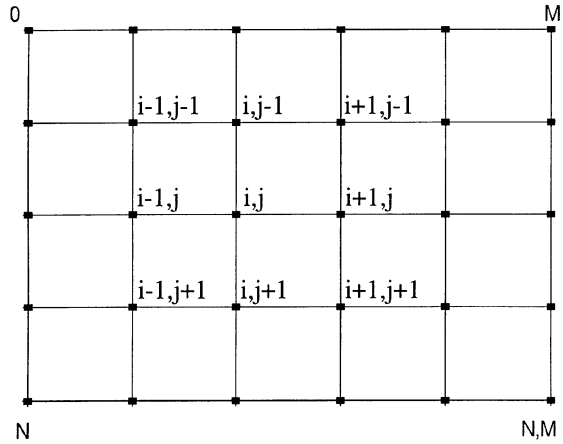


Figure 1 Iteration scheme.

the wave equation (3) is used to calculate the displacement at each gridpoint. The modulus of the displacement (u,v) is calculated at every grid point for each time increment. The "first arrival" of the wave is defined by the peak amplitude of the displacement modulus. ($\sqrt{[u^2+v^2]}$) Once an amplitude threshold is reached and the current value of the displacement modulus is less then the previous value, the location of the first arrival is marked. For a single time increment, the connection of all the first arrival locations constitutes the wavefront. With successive time steps the passage of the wave front through the specimen can be seen.

For selected time steps, the x,y coordinates for each grid point on the wavefront is tabulated. A central finite difference technique is used to find the slope of the wavefront at a particular point and the normal to the wavefront at that point is calculated. The normals are plotted for each layer and represent the raypaths through the specimen. The wave normals are compared to raypaths that are calculated from Snell's law and Fermat's principle using the known velocities.

## RESULTS AND DISCUSSION

The wavefronts for a single isotropic layer are shown in figure 2. As expected the wavefronts are circular due to the directional independence of the material properties. The data deteriorates near the upper edge and the sides of the specimen due to boundary effects. The circular wavefronts are within a cone shaped area in the center of the model. To avoid this problem, ray tracing was performed near the center portion of the data set.

The raypaths through a three layer medium are shown in figure 3. The velocity of the second layer is one half the velocity of the first and third layers, with all other material properties held constant. The raypath represents the normal to the wavefront calculated from a central finite difference numerical differentiation of the data. Snell's law has been calculated for each layer.

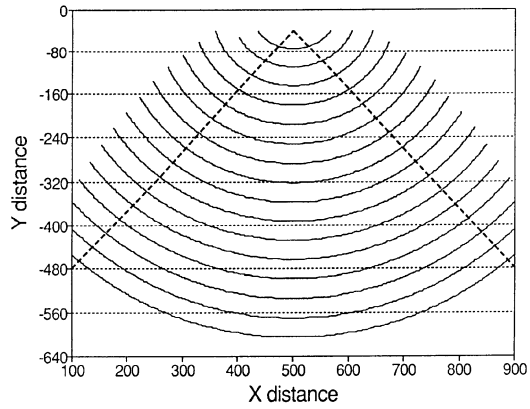


Figure 2 Wavefronts through a homogeneous medium. Inside cone, the wavefronts are circular.

$$\frac{\sin\theta_i}{v_i} = \frac{\sin\theta_{i+1}}{v_{i+1}} \tag{5}$$

where

$\theta_i$ = angle of incidence
$v_i$ = velocity of layer i

The calculated changes in wave normal for the Connection Machine displacements across a material discontinuity show good agreement with Snell's law. The slight discrepancies are the result of the error in the numerical differentiation. This could be improved with a smaller grid size.

Figure 4 depicts a raypath through an isotropic Epstein layer. The velocity increases linearly through eight layers from 2.5 m/s to 6.0 m/s. All other material properties are held constant. The wave normal is compared to the raypaths calculated from Snell's law and Fermat's principle. The discrepancy in the upper layers is caused by the poor data quality in the first two layers. There is excellent agreement between the different methods through the lower portion of the model.

This problem can be solved by increasing the number of processors assigned to the first layer. Figure 5(a) is an enlargement of the first two layers shown in figure 4. The wave normals do not obey Snell's law as shown in the figure. In figure 5(b), the number of processors in the first layer has been increased from 80 to 200, and the calculated wave normals obey Snell's law.

## CONCLUSIONS

A method for acoustic ray tracing has been developed for an isotropic nonhomogeneous material. The passage of the wavefront through a two-dimensional material is well represented. A cone shaped boundary defines the area where the Connection Machine data is reliable and the wavefronts are represented as circles. Near the upper surface and the outer edge of the model, boundary effects can cause

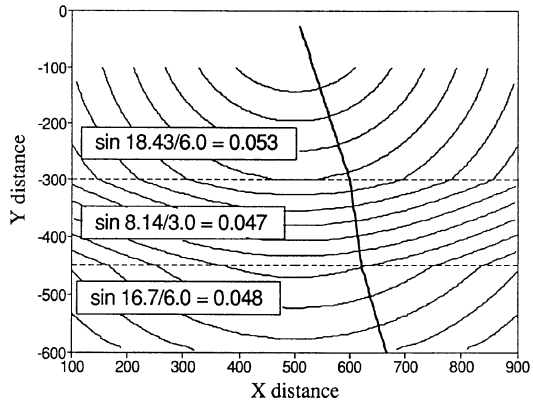


Figure 3 Wavefronts and a wave normal through a nonhomogeneous isotropic medium. Calculations for Snell's Law are shown for each layer.

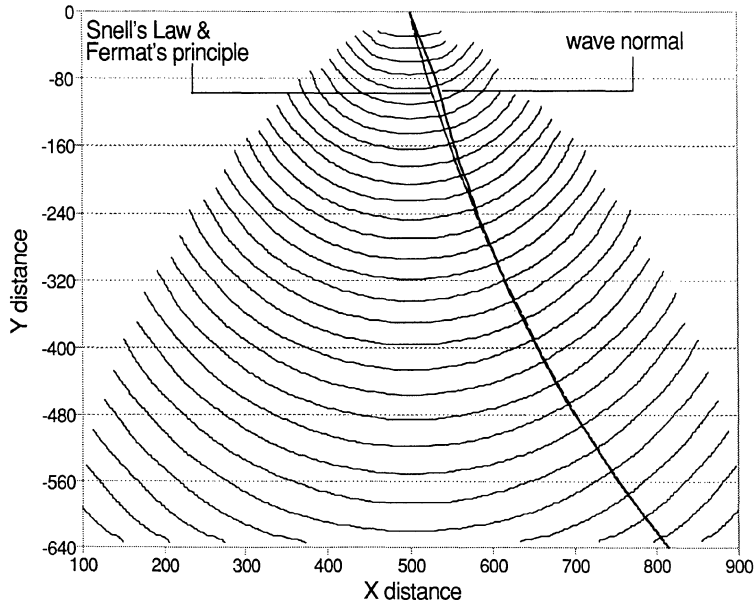


Figure 4 Wavefronts through an isotropic Epstein layer. The heavy line represents the wave normal and the thinner line is calculated from Snell's law and Femat's principle.

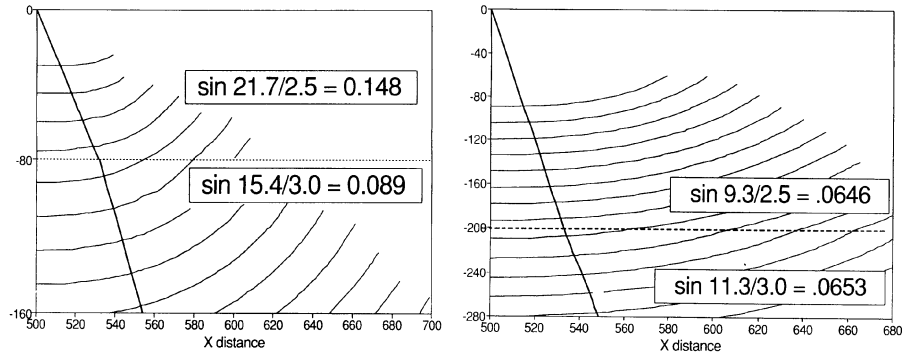


(a) (b)

Figure 5 (a) Enlarged view of the first 2 layers in figure 4. 80 processors were used in the first layer. (b) Same configuration as Fig. 5(a) except 200 processors were used in the first layer. Calculations for Snell's law are shown in both figures.

interference. To accurately predict the raypath, and avoid the boundary related effects, at least two hundred processors are required for the calculations in the first layer. The calculated changes in the normal to the wavefronts, within the cone shaped area of reliable data, agree with the raypaths calculated from Snell's law and Fermat's principle.

## ACKNOWLEDGEMENTS

This work is supported by the Naval Research Laboratory, Washington, D.C.

## REFERENCES

1. P.P. Delsanto, T. Whitcombe, H.H Chaskelis and R.B. Mignogna, in *Review of Progress in Quantitative NDE*, Vol. 9A, edited by D.O.Thompson and D.E. Chimenti (Plenum Press, New York, 1990) p.141
2. P.P. Delsanto, H.H Chaskelis and R.B. Mignogna, T. Whitcombe and R.S. Schechter, in *Review of Progress in Quantitative NDE*, Vol. 11A, edited by D.O.Thompson and D.E. Chimenti (Plenum Press, New York, 1991) p.113